Towards an experimental approach to KUBC homogenization

Thibault Dassonville[a,b,*], Martin Poncelet[b], Nicolas Auffray [a]

a. Université Paris-Est, Laboratoire de Modélisation et Simulation Multi Échelle
b. Université Paris Saclay, Laboratoire de Mécanique et de Technologie
* thibault.dassonville@u-pem.fr

Résumé :

Dans une pièce mécanique de multiples échelles coexistent, certains matériaux dits architecturés présentent une (voire plusieurs) échelle intermédiaire faiblement séparées de la structure globale. Cependant, inclure plus d'une échelle de manière directe dans une simulation demande des ressources numériques importantes. De nombreuses approches d'homogénéisation visant à contourner ce problème ont été développées, l'idée est de décrire de manière continue et macroscopique les effets dus à l'organisation de la matière aux échelles inférieures. Il est important de posséder des outils de vérification expérimentale des comportements déterminés numériquement.

Un dispositif permettant de déterminer le comportement élastique effectif d'un matériau architecturé est développé ici. L'idée a été d'adapter le schéma d'homogénéisation numérique de détermination par champ moyen en KUBC à un cadre expérimental. Un dispositif permettant de solliciter une éprouvette de 300x300mm^2 avec 10 points de contrôle par côté et 2 degrés de liberté par point de contrôle pour 2kN par côté a été conçu. Tout champ de déformation homogène du plan au bord d'un échantillon est applicable à l'aide de 5 actionneurs linéaires. Le déplacement est ensuite transmis et réparti grâce à un réseau 2D de pantographes placé autour de l'échantillon.

Abstract :

In a mechanical part, multiple scales coexist, some so-called architectured materials have one (or more) intermediate scale weakly separated from the global structure. However, including more than one scale directly in a simulation requires significant numerical resources. Many homogenization approaches have been developed to circumvent this problem. The idea is to describe in a continuous and macroscopic way the effects due to the organization of matter at the lower scales. It is important to have experimental verification tools for numerically determined behaviors.

A device for determining the effective elastic behavior of an architectured material is developed here. The idea was to adapt the numerical homogenization scheme by KUBC mean field to an experimental framework. A device for soliciting a specimen of 300x300mm^2 with 10 control points per side and 2 degrees of freedom per control point for 2kN per side has been designed. Any field of homogeneous plane strain at the boundary of a sample can be imposed by means of 5 linear actuators. The displacement is then transmitted and distributed through a 2D network of pantographs placed around the sample.

Mots clefs : homogenization, architectured materials, biaxial testing, rich boundary conditions.

1 Introduction

Architectured materials had open new areas in material properties spaces [1] and make it possible to respond to previously incompatible constraints such as low density and high strength. They are distinguished by the existence of at least one intermediate scale between the microscopic and the macroscopic ones. Historically, the development of the microstructure and its properties is the domain of metallurgists who works on the compositions and the characteristic lengths while the development of the macrostructure is the domain of mechanicians who play with the geometry. The development of architectured materials requires expertise in these two fields since all these parameters are controllable [2].

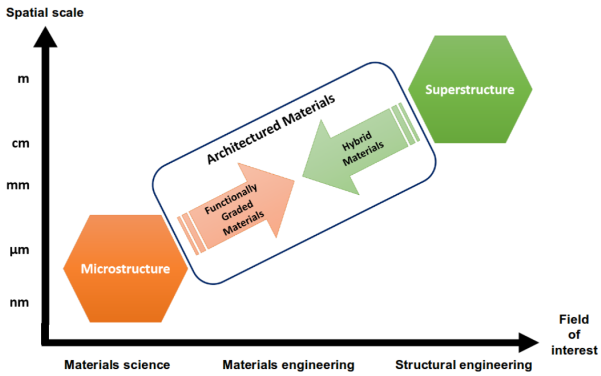

FIGURE 1 – Characteristic scales and related fields [3]

The existence of intermediate scales creates new challenges in numerical simulation. Hence, the necessity to take into account the coupled behavior of the material and the geometry increases the calculation cost, which can be prohibitive in an optimization approach for example. To circumvent these difficulties, a possible way is to substitute the actual material by an homogeneous one having equivalent effective properties. In the context of linear elasticity, to which this paper is devoted, the goal is to define the apparent tensor $\underset{\approx}{C}^\star$ which, over a RVE, relates the average volume strain ($\underset{\sim}{E}$) to the average volume stress($\underset{\sim}{\Sigma}$) :

$$\underset{\approx}{C}^\star : \underset{\sim}{E} = \underset{\sim}{\Sigma}$$

$\underset{\sim}{\varepsilon}(\underset{\sim}{x})$, $\underset{\sim}{\sigma}(\underset{\sim}{x})$ being the average tensors defined by

$$\underset{\sim}{E} = \langle \underset{\sim}{\varepsilon}(\underset{\sim}{x}) \rangle = \frac{1}{V} \int_\Omega \underset{\sim}{\varepsilon}(\underset{\sim}{x}) \ \mathrm{d}V \quad ; \quad \underset{\sim}{\Sigma} = \langle \underset{\sim}{\sigma}(\underset{\sim}{x}) \rangle$$

Two main types of periodic architectured materials can be distinguished [4] : lattice materials and periodic blocks. Lattices materials are composed of thin elements joint together, consisting of a large proportion of empty space. Periodic blocks are, on the other hand, fully dense, the architectured is given by material contrast. Recent advance in additive manufacturing techniques allow a fast and simple production of lattices which lead to a large renewed interest in it.

However, geometrical and material qualities obtained by additive manufacturing techniques remain poor and are very variable depending on the printing technique [5, 6], printer characteristic [7], orientation [8] and even position on printer table [8]. Thus, it is necessary to complete numerical studies by experimental tests to fully characterized a sample of architectured material. But no standard test has been found to determine completely and directly the effective behaviour of a material.

The purpose of this work is to present a homogenization technique in linear elasticity for architectured materials by a fully experimental process.

2 Numerical homogenization

If many theoretical [9] and numerical [10, 11, 12] schemes of homogenization has been developped for specific fields, static, dynamic, linear or non linear elasticity, a very few of them are transposable to a realistic experimental setting. Indeed, volume loadings and measurements will be put aside, because of the complexity of their implementation in an experimental setting. Considering this, strategies based on the use of boundary conditions seem to be the moste likely transposable. They are known as kinematic uniform (KUBC), static uniform (SUBC) and periodic (PBC). The last one gives exact results while KUBC and SUBC give overestimated and underestimated apparent rigidity. The apparent behaviour depends on the number of unit cells and converge to the effective behaviour [13]. PBC being hard to apply, the choice is made to turn to a KUBC process.

2.1 Sample description

The sample of architectured material we intent to determine the homogenized behaviour is supposed to be filled by two elastic materials. The characteristic length scales of the problem are defined in fig. 2. The macroscopic length L and the mesoscopic one l will be considered thereafter while the microscopic length λ will be put aside. Only the plane behaviour will be treated.

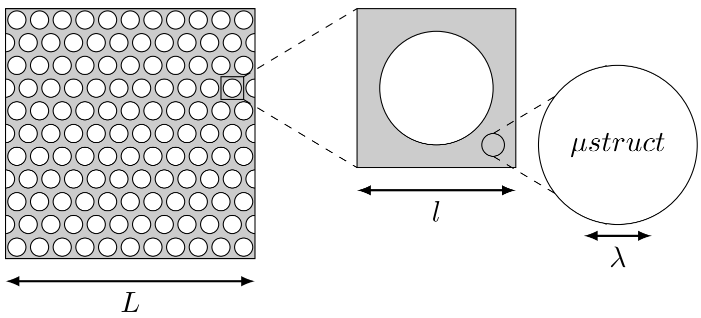

FIGURE 2 – Sample and characteristic length

2.2 Numeric KUCB homogenization

Fulfiling the homogenization of a linear elastic material by a KUBC method is looking for $\underset{\approx}{C}^\star$ such as : $\underset{\sim}{\Sigma} = \underset{\approx}{C}^\star : \underset{\sim}{E}$. Using de Kelvin notation, second order tensor in $\mathbb{R}^2$ can be turned into vector in $\mathbb{R}^3$.

$$[\hat{\underset{\sim}{E}}] \quad ; \quad [\hat{\underset{\sim}{\Sigma}}] \quad ; \quad [\hat{\underset{\approx}{C}}^*]$$

Where $[\,\cdot\,]$ is the matrix notation of the tensorial quantity $\cdot$ and $\hat{\cdot}$ it's the de Kelvin notation. The principle of mean field homogenization is as follows [10]. Consider a mean state of strain $\underset{\sim}{E}$ and stress $\underset{\sim}{\Sigma}$, and decompose them over the cardinal basis of $\mathbb{R}^3$:

$$\hat{\underline{E}} = \hat{E}_i \hat{\underline{e}}_i \quad , \quad \hat{\underline{\Sigma}} = \hat{\Sigma}_i \hat{\underline{e}}_i$$

We have

$$\hat{C}_{ij} = \hat{\underline{e}}_i \cdot \hat{\underline{\Sigma}}^{\mathbb{1}}_j \qquad \text{With} \quad \hat{\underline{\Sigma}}^{\mathbb{1}}_i = \hat{\underset{\sim}{C}} \cdot \hat{\underline{e}}_i$$

or, more explicitly

$$[\hat{\underset{\sim}{C}}] = \begin{pmatrix} \hat{\underline{\Sigma}}^{\mathbb{1}}_1 \cdot \hat{\underline{e}}_1 & \hat{\underline{\Sigma}}^{\mathbb{1}}_2 \cdot \hat{\underline{e}}_1 & \hat{\underline{\Sigma}}^{\mathbb{1}}_3 \cdot \hat{\underline{e}}_1 \\ \hat{\underline{\Sigma}}^{\mathbb{1}}_1 \cdot \hat{\underline{e}}_2 & \hat{\underline{\Sigma}}^{\mathbb{1}}_2 \cdot \hat{\underline{e}}_2 & \hat{\underline{\Sigma}}^{\mathbb{1}}_3 \cdot \hat{\underline{e}}_2 \\ \hat{\underline{\Sigma}}^{\mathbb{1}}_1 \cdot \hat{\underline{e}}_3 & \hat{\underline{\Sigma}}^{\mathbb{1}}_2 \cdot \hat{\underline{e}}_3 & \hat{\underline{\Sigma}}^{\mathbb{1}}_3 \cdot \hat{\underline{e}}_3 \end{pmatrix} \tag{1}$$

Hence the theoretical determination of a column of $[\hat{\underset{\sim}{C}}]$ is a three-step process :

1. Imposing a mean strain state $\hat{\underline{e}}_i$ over the whole domain Ω ;
2. Measuring the resulting stress field $\hat{\underset{\sim}{\sigma}}^{\mathbb{1}}(\underline{x})$;
3. Computing the mean stress field $\hat{\underset{\sim}{\Sigma}}^{\mathbb{1}}$ and the associated dot products.

3 Experimental homogenization

In order to fulfill a KUBC homogenization scheme in an experimental context two main problems arise

— Apply kinematic uniform boundary conditions on a sample ;

— Determine the value of the macroscopic stress $\underset{\sim}{\Sigma}$.

This section is organized as an answer to these questions. First, the global concept of a device capable of applying KUBC is discussed. Then a method for determining the mean stress field is presented.

3.1 Machine type

The first challenge consists in imposing a uniform kinematic, two types of solutions can be considered. On the one hand, an actuator can be devoted to each degree of freedom (dof) of each control point on the boundary (fig. 3a), this solution will be called local. On the other hand, an actuator can be devoted to impose the kinematic of a whole edge, in this case a mechanical device is interposed between the actuator and the sample to distribute the displacement (fig. 3b), this solution will be called global.

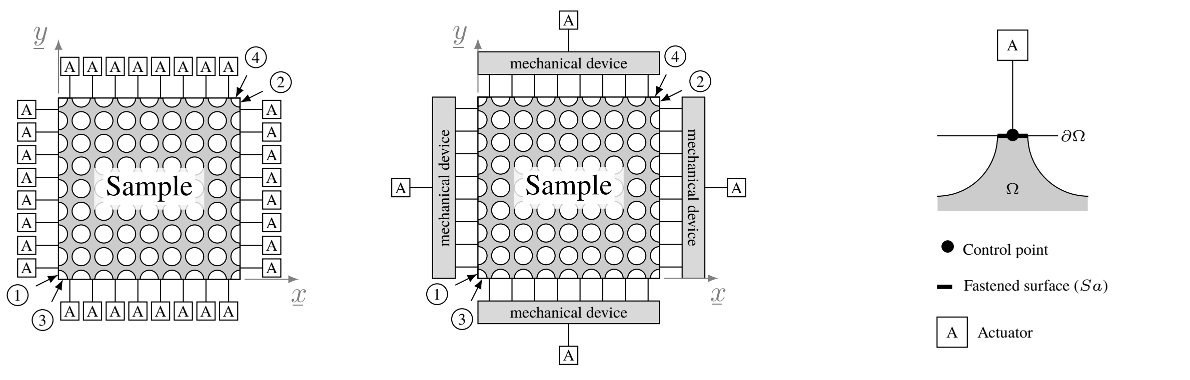

(a) Local type machine (b) Global type machine (c) Local description

FIGURE 3 – Schematic diagramm of local and global type devices

The two approaches seem reasonable and both have strengths and weaknesses in term of in costs, bulkiness, ease of use and versatility but the global one seems more elegant to our eyes. Only this idea will be studied thereafter.

3.2 Feasability of experimental homogenization

If the determination of $\hat{\underset{\sim}{\Sigma}}$ is esay to achieve in a numerical situation, this is not the case in an experimental setting. Indeed to do this, the field $\hat{\underset{\sim}{\sigma}}(\underline{x})$ has to be known which is not generally speaking possible in an experimental setting. It must therefore be determined with information poorer than the knowledge of the field in every point. First, with the divergence theorem the average operation can be projected on the edges

$$V\underset{\sim}{\Sigma}\int_{\Omega}\underset{\sim}{\sigma}(\underline{x})\,\mathrm{d}V=\int_{\partial\Omega}(\underset{\sim}{\sigma}(\underline{x})\cdot\underline{n})\otimes\underline{x}\;\mathrm{d}S$$

In our case, the edge is divided into 2 subsets corresponding to the two phases : material and void (stress free). And the material subset is divided into several fastened surfaces. So the integral can be split as follows with $4N$ the number of fasteners on $\partial\Omega$ and $\partial\Omega_p$ the restriction of $\partial\Omega$ to one fastener. A quantity denoted $\cdot^{\,p}$ refers to the quantity restricted to the p fastener.

$$V\Sigma_{ij}=\sum_{p=1}^{4\,N}\int_{\partial\Omega^p}\sigma_{ik}^{p}\,x_j^p\,n_k^p\;\mathrm{d}S$$

If we consider that the fasteners are sufficiently narrow so that the fields are locally homogeneous :

$$\sigma_{ik}^{p}(\underline{x})=\sigma_{ik}^{0p}$$

we get :

$$V\Sigma_{ij}=\sum_{p=1}^{4N}S^p\,\sigma_{ik}^{p}\,x_j^p\,n_k \tag{2}$$

The previous sum eq. (2) can be splited on the four edges of the sample with specific expressions of $\underline{n}$ and $\underline{x}$. A quantity denoted $\cdot^{\,sp}$ refers to the quantity restricted to the p fastener of the s edge of the sample. Finally

$$\underset{\sim}{\Sigma}=\frac{1}{V}\begin{pmatrix}\sum_{p=1}^{N}\left(L\,f_x^{2p}-x^p\,f_x^{3p}+x^p\,f_x^{4p}\right) & \sum_{p=1}^{N}\left(-y^p\,f_x^{1p}+y^p\,f_x^{2p}+L\,f_x^{4p}\right)\\ \sum_{p=1}^{N}\left(L\,f_y^{2p}-x^p\,f_y^{3p}+x^p\,f_y^{4p}\right) & \sum_{p=1}^{N}\left(-y^p\,f_y^{1p}+y^p\,f_y^{2p}+L\,f_y^{4p}\right)\end{pmatrix} \tag{3}$$

with $f_j^{sp}=S^p\,\sigma_{jk}^{sp}\,n_k^s$ the j component of the effort on the pth fastener of the edge s. The value of these sums remains to be determined. Half of them are easy to, they are just the resultant forces on one edge.

The other half is not as direct but Castigliano's theorem gives :

$$\sum_{p=1}^{N} x^p \, f_x^{sp} = \sum_{p=1}^{N} L \, f_x^{sp} = L \, F^s \tag{4}$$

Each term of $\hat{\Sigma}$ can be computed only with the information of the resultant forces on the edges. The equality eq. (4) has been obtained for a mechanical device (fig. 3b) with zeros strain energy.

4 Design of the device

Considering that the resultant forces on the edges are enough to determine $\hat{\Sigma}$, a device with few actuators and a repartition structure seems relevant. The main key is to have a repartition device (fig. 3b) with zero strain energy which ensures a displacement proportional to the position (KUBC) :

$$\underline{u}(\underline{x}) = \underset{\sim}{E} \cdot \underline{x}$$

A well known structure with these characteristics is the pantograph (fig. 4). This structure material is made of rigid bars and pivots. The extension - compression of the structure is a soft mode : no strain energy is associated to it. All other modes involve the stiffness of the bar, so that imposing the kinematic of two joints amounts to impose the kinematic of the whole structure, the displacement of a joint between the two imposed is the average weighted by the distance of the two imposed displacements. For example on fig. 4 if the bottom left joint (in green) is fixed and chosen for axis origin and the displacement of the bottom right joint (in red) is imposed to $\underline{u} = a\underline{x}$. The joints between them will have an imposed kinematic $\underline{u} = \frac{a}{L}\underline{x}$, which is exactly a discretized kinematic uniform condition.

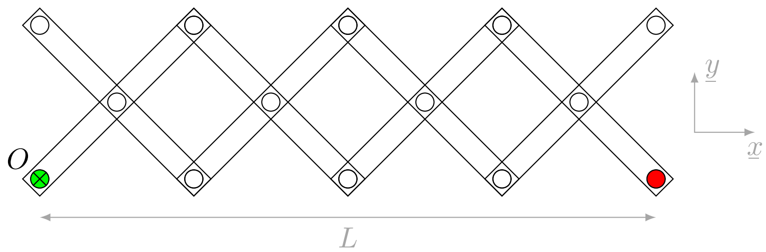

FIGURE 4 – Schematic diagramm of a pantograph

Thereby, the use of a pantographic frame around a sample controlled by five actuators (fig. 5) will guarantee discretized KUBC conditions on the sample. Such uses of pantographic frames can be found in the litterature [14] or in industrial context (Accupull) but not with the same scope, and consequently not the same features, as in the present study

One of the major disadvantage of a pantographic structure is the high number of pivots, which leads to friction and bending of the pantograph due to the clearance. Both are critical for such a device, bending of the pantograph induces kinematic error, while friction in the links generates not determinable forces which interferes with the global measurement. To overcome this, classical pivots will be replaced by flexible links (fig. 6) for which the rotation is ensured by elastic strain of the link, so that no clearance or friction remain.

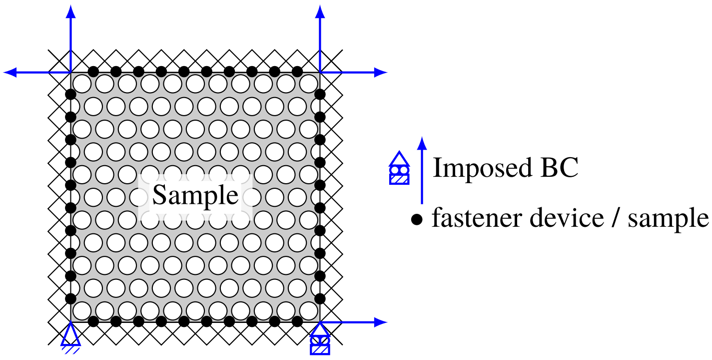

FIGURE 5 – Field application device by pantographic frame

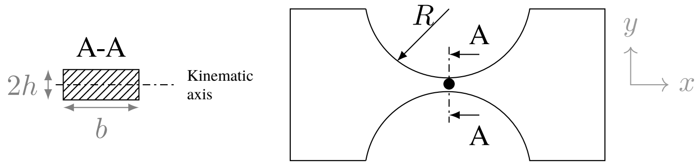

FIGURE 6 – Description of a flexible link and its minimum section

However, these links admit limited rotation and charges so that we have to size them carefully. In order to do that a finite element code with macro-elements describing the behaviour of a whole arm has been developed. This allows to easily compute the behaviour of the complete device composed of a large number of arms. Finally, a more complex structure is obtained with multiple rows pantographs (the arms have more than three pivot links) and two pantographic frames, put face to face the sample between them to avoid off plane effects (fig. 7).

5 Conclusion

In this work, the possibility of carrying out a process of homogenization by KUBC of an architectured material in an experimental setting has been discussed. A method of determining the average stress field on the volume with reasonable measuring means is presented. Finally, a proposal of a mechanical system for effectively applying KUBC to a sample is disclosed. The numerical description of the device will be useful for designing the experiments. Machining and making of the device are still to be done. Then a first characterisation work will have to be carried out to determine the exact behaviour of the machine before any homogenization attempt.

Références

[1] Fleck N. A., Deshpande V. S., and Ashby M. F. Micro-architectured materials : past, present and future. *Proceedings of the Royal Society A : Mathematical, Physical and Engineering Sciences*, 466(2121) :2495–2516, September 2010.

[2] O. Bouaziz, Y. Bréchet, and J. D. Embury. Heterogeneous and Architectured Materials : A Possible Strategy for Design of Structural Materials. *Advanced Engineering Materials*, 10(1-2) :24–36, 2008.

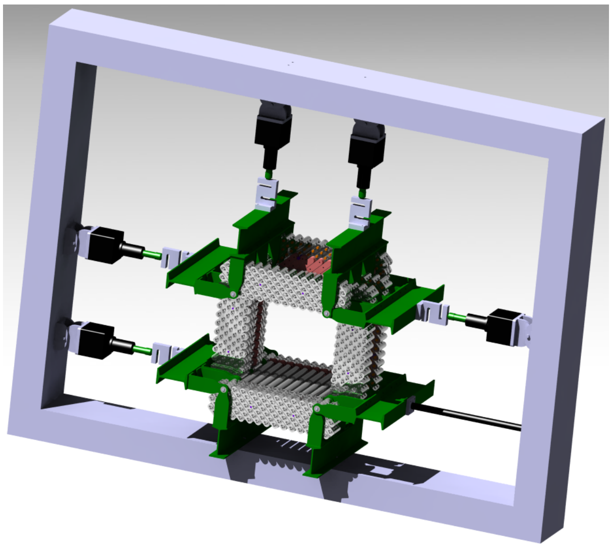

Figure 7 – CAD view of the complete device

[3] Justin Dirrenberger. Towards an integrated approach for the development of architectured materials. December 2018.

[4] F. Barthelat. Architectured materials in engineering and biology : fabrication, structure, mechanics and performance. *International Materials Reviews*, 60(8) :413–430, November 2015.

[5] Mamta Juneja, Niharika Thakur, Dinesh Kumar, Ankur Gupta, Babandeep Bajwa, and Prashant Jindal. Accuracy in dental surgical guide fabrication using different 3-D printing techniques. *Additive Manufacturing*, 22 :243–255, August 2018.

[6] Wen See Tan, Stanislaus Raditya Suwarno, Jia An, Chee Kai Chua, Anthony G. Fane, and Tzyy Haur Chong. Comparison of solid, liquid and powder forms of 3d printing techniques in membrane spacer fabrication. *Journal of Membrane Science*, 537 :283–296, September 2017.

[7] B. M. Tymrak, M. Kreiger, and J. M. Pearce. Mechanical properties of components fabricated with open-source 3-D printers under realistic environmental conditions. *Materials & Design*, 58 :242–246, June 2014.

[8] Michael Barclift and Christopher Williams. Examining variability in the mechanical properties of parts manufactured via polyjet direct 3d printing. *23rd Annual International Solid Freeform Fabrication Symposium - An Additive Manufacturing Conference, SFF 2012*, January 2012.

[9] Grégoire Allaire and Marc Schoenauer. Conception optimale de structures. volume 58, pages 163–175. Springer, 2007.

[10] Michel Bornert, T. Bretheau, and P. Gilormini. *Homogénéisation en mécanique des matériaux, Tome 1 : Matériaux aléatoires élastiques et milieux périodiques*. Hermes science, 2001.

[11] H. Moulinec and P. Suquet. A numerical method for computing the overall response of nonlinear composites with complex microstructure. *Computer Methods in Applied Mechanics and Engineering*, 157(1) :69–94, April 1998.

[12] Frédéric Feyel. Multiscale FE2 elastoviscoplastic analysis of composite structures. *Computational Materials Science*, 16(1-4) :344–354, December 1999.

[13] P. M. SUQUET. Elements of Homogenization for Inelastic Solid Mechanics, Homogenization Techniques for Composite Media. *Lecture Notes in Physics*, 272 :193, 1985.

[14] Hackmet Aly Joer. *" 1 [gamma] 2 [epsilon]" : une nouvelle machine de cisaillement pour l'étude du comportement des milieux granulaires*. PhD Thesis, Université Joseph Fourier, 1991.